C. R. Physique 12 (2011) 817–825

Contents lists available at SciVerse ScienceDirect

Comptes Rendus Physique

www.sciencedirect.com

Nano- and micro-optomechanical systems / Nano- et micro-résonateurs optomécaniques

dc SQUIDs as linear displacement detectors for embedded micromechanical resonators

Détection linéaire des déplacements d'un microrésonateur mécanique à l'aide d'un SQUID

Samir Etaki [a,b,*], Menno Poot [a], Koji Onomitsu [b], Hiroshi Yamaguchi [b], Herre S.J. van der Zant [a]

[a] *Kavli Institute of Nanoscience, Delft University of Technology, P.O.B. 5046, 2600GA Delft, The Netherlands*
[b] *NTT Basic Research Laboratories, NTT Corporation, Atsugi-shi, Kanagawa 243-0198, Japan*

ARTICLE INFO

Article history:
Received 12 November 2010
Accepted after revision 10 October 2011
Available online 9 November 2011

Keywords:
NEMS
MEMS
QEMS
SQUID

Mots-clés :
NEMS
MEMS
QEMS
SQUID

ABSTRACT

Superconducting quantum interference devices (SQUIDs) can detect tiny amounts of magnetic flux and are also used to study macroscopic quantum effects. We employ a dc SQUID as a linear detector of the displacement of an embedded micromechanical resonator with a femtometer sensitivity. We discuss the measurement method, including operation in high magnetic field and a cryogenic amplification scheme which allows us to reach a resolution which is only a factor 4.4 above the standard quantum limit.

RÉSUMÉ

Les magnétomètres à base de SQUID (Superconducting QUantum Interference Device) sont sensibles à de très faibles variations de flux magnétique et sont ainsi utilisés pour l'étude d'effets quantiques à l'échelle macroscopique. Nous avons réalisé une mesure linéaire du déplacement d'un microrésonateur mécanique enchâssé dans la boucle supraconductrice d'un dc SQUID. En utilisant un fort champ magnétique et un amplificateur fonctionnant en régime cryogénique, cette méthode de mesure nous a permis d'atteindre une résolution qui n'est que 4,4 fois la limite quantique.

1. Introduction

1.1. Mesoscopic mechanics

Mechanical resonators are used as sensitive detectors of forces. Although they are typically macroscopic structures consisting of many atoms and thus have many degrees of freedom, the eigenmodes with the lowest energies can be engineered to be almost completely isolated from all other modes, even at the micro- and nanometer scale [1]. These modes then act as one-dimensional harmonic oscillators. They can store mechanical energy for long times and react with a large change in oscillation amplitude or resonance frequency to any applied force. The fundamental limits to the noise added by these resonant mechanical force detectors to the force to be measured was explored early on by the gravitational wave community [2].

* Corresponding author at: Kavli Institute of Nanoscience, Delft University of Technology, P.O.B. 5046, 2600GA Delft, The Netherlands.
E-mail address: etaki@hotmail.com (S. Etaki).

1631-0705/$ – see front matter
doi:10.1016/j.crhy.2011.10.005

The mean-square displacement due to stochastic force noise is related to the potential energy of the resonator $\frac{1}{2}k_R\langle u^2\rangle$, where k_R is the spring constant of the resonator mode and u is the displacement of the resonator with respect to its equilibrium position. It is known from statistical mechanics that the expectation value for the potential energy in a harmonic oscillator with frequency f_R at temperature T_R is

$$\frac{1}{2}k_R\langle u^2\rangle = \frac{1}{2}hf_R\left(\frac{1}{2} + \frac{1}{e^{\frac{hf_R}{k_BT_R}} - 1}\right) \tag{1}$$

At temperatures for which the thermal energy is much larger than the energy of a single phonon, i.e. $k_BT_R \gg hf_R$, this expression reduces to the equipartition theorem

$$\frac{1}{2}k_R\langle u^2\rangle = \frac{1}{2}k_BT_R \tag{2}$$

At absolute zero the only fluctuations that remain are the zero-point fluctuations with an average energy of half a phonon. In order to use the resonator as a force sensor its displacement must be detected, typically by conversion to an output voltage. If the position detector couples linearly to the deflection of the resonator, quantum mechanical analysis shows that even an ideally coupled, quantum limited detector adds at least another half a phonon of noise energy [2,3]. This can be understood as the contribution of the internal degrees of freedom in the detector when they are coupled to the resonator. The total added noise consists of the imprecision noise of the detector, which shows as a white displacement noise floor at the detector output and the back action force noise, which increases the amplitude of the Lorentzian noise peak of the resonator. In this article only the detector resolution due to measurement imprecision is discussed, back-action noise is not included. Although the resolution can be made arbitrarily small by increasing the coupling between the detector and the resonator, the optimum coupling will yield a resolution on the order of the zero-point motion of the resonator:

$$\sqrt{\langle u^2\rangle_{QL}} = \sqrt{\frac{hf_R}{2k_R}} \tag{3}$$

This is the mean-square displacement associated with half a phonon and is known as the standard quantum limit. Note that these fluctuations only become significant once the resonator is cooled to a temperature such that $k_BT \ll hf_R$.

Position measurements of micro- and nanomechanical resonators in the quantum regime are of interest not only because they reveal the quantum nature of a massive, macroscopic degree of freedom; a ground-state cooled resonator can also be prepared in a non-classical state and subsequently used to transfer that state to for example a quantum information element [4]. Resonators which are coupled to mesoscopic electronics allow investigation of the interaction between their respective degrees of freedom. The resulting interesting physics has been investigated for devices such as the Single-Electron Transistor (SET) [5,6], the Atomic Point Contact (APC) [7] and the Quantum Point Contact (QPC) [8]. Although most of these devices have the potential for resolution beyond the quantum limit, optomechanical [9] and electromechanical [10] cavity resonators are among the first micro-scale systems to reach this milestone.

We use a Superconducting Quantum Interference Device (SQUID) to detect the position of an integrated microresonator. SQUIDs are an important class of mesoscopic detectors which are primarily used for the detection of tiny magnetic fields [11]. We use a magnetic field to couple the position of the integrated resonator to the flux that threads the loop. In previous work, we achieved a position resolution of a factor 36 above the quantum limit for linear position detection [12]. In this article we focus on the position detection in more detail. We explain the measurement setup and electronics in more detail and we report on improvements which have resulted in an order-of-magnitude improvement in the resolution to 4.4 times the standard quantum limit.

1.2. The dc SQUID position detector

We start with a short explanation of the operating principle of the dc SQUID (Fig. 1). A more comprehensive description can be found in [11]. The basic element of the dc SQUID is the Josephson junction, through which supercurrent can flow up to a maximum (critical) value I_0. For bias currents I_B beyond I_0, a voltage develops across the junction due to a quasiparticle current which runs through the normal-state resistance R of the junction.[1]

A dc SQUID consists of two Josephson junctions in parallel inside a superconducting loop which is contacted by two leads. Due to the condition of phase continuity of the Cooper pair wave function around the loop, a supercurrent J will run around the loop in response to an applied magnetic flux Φ through the inner part of the SQUID loop. The result is that the dc SQUID acts as a single Josephson junction with a critical current I_C which can be tuned between the sum of the critical current of the two junctions, $I_C^{\mathrm{MAX}} = I_{0,1} + I_{0,2}$ and their difference $I_C^{\mathrm{MIN}} = |I_{0,1} - I_{0,2}|$ by changing Φ by half a flux quantum, $\Phi_0 = h/2e = 2$ fTm^2. Φ_0 is a tiny amount of magnet flux and this is the reason why the SQUID has a high flux

[1] The device in this article is overdamped, which means that the V_{SQ}–I_B curves are non-hysteretic. This is a necessary condition for using the SQUID as a continuous linear flux detector above its critical current, i.e. in the dissipative regime [11].

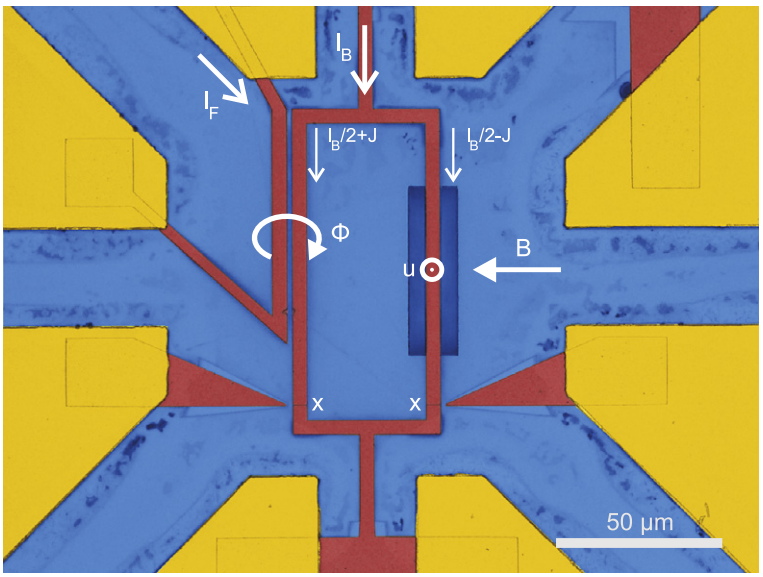

Fig. 1. Colored SEM image of the dc SQUID, which consists of a 40 × 80 μm niobium loop with 4.5 μm wide arms (red), interrupted by two 300 nm long indium arsenide junctions (marked X), contacted by gold pads (yellow) and situated on an insulating AlGaSb-on-GaAs substrate (blue) [19]. The mechanical resonator has length $\ell = 50$ μm. It is defined by two windows which are etched through the AlGaSb into the GaAs (dark blue) and it is suspended by removing the underlying GaAs. The resonator has a fundamental mode which moves perpendicular to the substrate plane with a coordinate u, whose displacement is equal to the root-mean-squared displacement of the beam averaged over the beam's length.

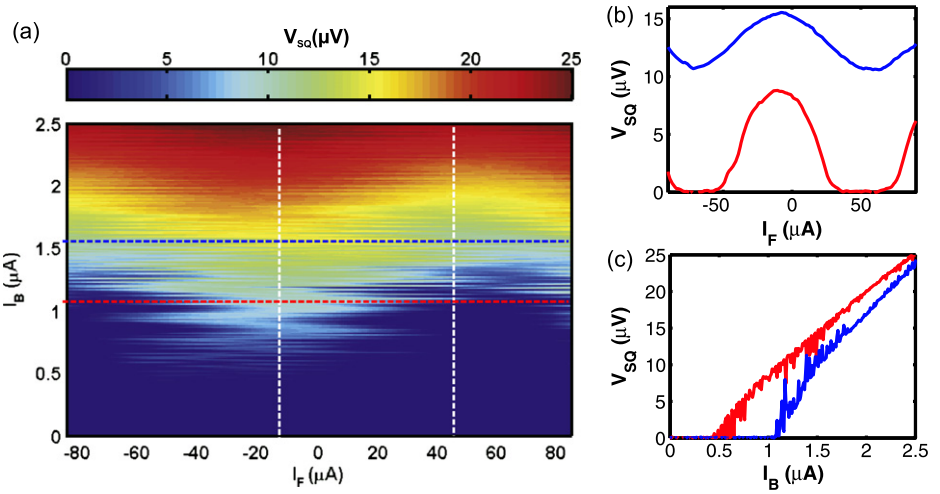

Fig. 2. (a) Measured dc SQUID output voltage V_{SQ} as a function of bias current I_B and stripline current I_F. In the blue region the SQUID is superconducting. The critical current varies periodically. A current of 125 μA through the stripline changes Φ by one flux quantum, which yields a mutual inductance $M_{STRIP} = \Phi_0/\Delta I_F = 16$ pH between the stripline and the SQUID loop. (b) V_{SQ} versus I_F for two values of I_B (horizontal dashed lines in (a)). (c) V_{SQ} versus I_B for two values of I_F: Left vertical white line in figure (a) corresponds to the red curve, the right line corresponds to the blue curve. The visible fluctuations are due to flux interference. Note that the feedback loop which stabilizes the flux is not engaged during this measurement. On the other hand, it is always used during measurements on the mechanical resonator.

sensitivity. If the SQUID is biased above I_C, a voltage V_{SQ} develops which also depends on Φ, making the SQUID a linear flux detector for flux signals which are much smaller than Φ_0. The flux responsivity is then defined as $V_\Phi = \frac{\partial V_{SQ}}{\partial \Phi}$, which is tunable by Φ and I_B. Φ is controlled by applying a current I_F through a stripline next to the SQUID (see Fig. 1).

Fig. 2 shows the relationship between V_{SQ}, I_B and I_F as measured for the device in this article. The device behavior is consistent with the resistively shunted Josephson junction (RCSJ) model [11]. The largest values for V_Φ are obtained for $I_B < I_C^{MAX}$ and $V_{SQ} \to 0$ V (Fig. 2(b)). In fact, in a noiseless SQUID model, V_Φ goes to infinity for $V_{SQ} \to 0$. Flux noise however strongly decreases the gain in this region, and this is why the maximum gain is found above $V_{SQ} = 0$.

A description of the device is given in Fig. 1. In order to use the dc SQUID as a displacement detector, a section of the loop forms a freely suspended beam and the SQUID is placed in a magnetic field B which is parallel to the substrate plane and perpendicular to the length direction of the beam. In this way, Φ changes when the beam displaces. The displacement

u of the fundamental eigenmode is defined as the root-mean-square (RMS) displacement of the modeshape $u(x)$ along the length ℓ of the beam,

$$u = \left(\ell^{-1} \int_0^\ell u(x)^2 \, \mathrm{d}x \right)^{1/2} \tag{4}$$

With this definition, the spring constant of the mode is $k_R = m(2\pi f_R)^2$, where m is the total mass of the beam. The displacement u causes a change in flux of $aB\ell u$, where

$$a = (u\ell)^{-1} \int_0^\ell u(x) \, \mathrm{d}x \tag{5}$$

is the normalized change in loop area. For the fundamental mode of the buckled beam, $a \approx 0.9$ [12]. If the SQUID is biased above I_C, it can thus act as a linear transducer for the motion of the beam with a responsivity

$$\frac{\partial V_{SQ}}{\partial u} = G_{HF} V_\Phi a B \ell \tag{6}$$

where G_{HF} is the gain of the high-frequency voltage amplifier which is discussed in the next section. In order to have a large responsivity, it would seem that the largest possible B field is preferable. This is, however, not true, because the critical current of the junctions and thus also the flux gain V_Φ decrease rapidly for fields on the order of 100 mT due to flux vortex formation [12]. All the measurements in this paper are performed at $B = 60$ mT, where the optimal displacement responsivity was found for this device.

The motion of the resonator can be detected either by measuring the thermal and/or quantum mechanical position fluctuations using a spectrum analyzer or by measuring the response of the resonator due to a driving force using a network analyzer. To perform the driven measurement with the network analyzer, the resonator is mounted on a piezo actuator which moves the entire substrate perpendicular to the substrate plane, thereby actuating the resonator. Using a driven measurement, the fundamental resonance frequency f_R of the beam is found at 2.1385 MHz. The beam has a calculated total mass $m = 6 \times 10^{-13}$ kg [12], which gives a spring constant $k_R = 110$ N/m. The resonator has a quality factor $Q_R = 3 \times 10^4$ at 15 mK. Note that at this temperature, the resonator is far in the limit $k_B T_R / h f_R > 100$, where equipartition applies (Eq. (2)).

Due to the applied magnetic field, the circulating current J exerts a Lorentz force on the resonator which is proportional to its displacement and its velocity. This back-action causes a tunable shift in the resonance frequency and damping rate of the resonator, as we have measured recently [13]. Back-action may also enable cooling below the environmental temperature [14]. For the device in this article, the back-action is disregarded, as it is weak and the experiments are conducted at a SQUID bias where its effects cannot be detected.

2. Measurement setup

Fig. 3 shows the physical setup and Fig. 4 shows a schematic of the measurement electronics. In this section we address the two main measurement issues, which are the low-noise amplification of the dc SQUID output voltage and the stabilization of the magnetic flux in the SQUID loop while operating it in a relatively large magnetic field.

2.1. Vibration control

Optimization of displacement detection requires a constant average magnetic flux in the SQUID loop. This is a highly nontrivial task since small vibrations of the superconducting magnet with respect to the SQUID can already cause changes in the magnetic flux through the SQUID loop of the order of Φ_0. To clarify this point, we must examine the setup in more detail. The device is connected to a cold finger which in turn is connected to the mixing chamber of a dilution refrigerator. Fig. 3 shows the physical situation. The dilution unit is mounted at the end of a 5 cm diameter dipstick which is hanging in a dewar of liquid helium. The dipstick is supported only at the neck of the dewar and is therefore able to vibrate in directions perpendicular to its length. The superconducting magnet on the other hand is suspended separately in the dewar. Considering the inner area of the SQUID loop, 40×80 (μm)^2, a free length of 1 m for the dipstick and a typical coupling field of 60 mT, a simple geometrical calculation yields a flux change of 1 Φ_0 for every 10 μm of lateral displacement of the end of the dipstick. Because of this extreme sensitivity to vibrations, the dewar is placed on a damped platform. It damps most strongly in the direction of the pumping lines coming from the gas handling system, as they are the strongest source of vibrations. Nevertheless, the remaining RMS amplitude of the vibration-induced flux interference is around $0.5\Phi_0$ up to 1 kHz.

In order to further stabilize the amount of magnetic flux in the loop, we employ a proportional-integral feedback loop which controls the current through the stripline to maintain a constant voltage setpoint, V_{SP}, across the SQUID. Before operating the feedback loop, all electronic interference which is not related to the magnetic flux must be removed, as it

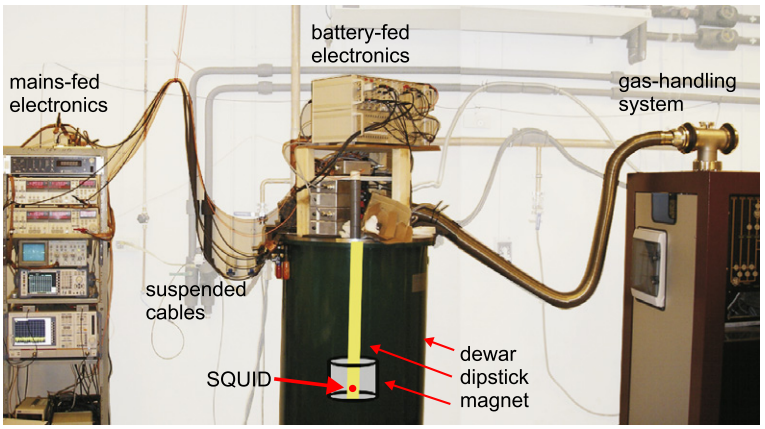

Fig. 3. The physical setup consists of the SQUID which is mounted on a dipstick-sized dilution refrigerator and placed in a helium dewar with a superconducting magnet to provide the magnetic field B. The SQUID is connected to custom-built, battery fed control and readout electronics which are optically isolated from the mains-fed measurement equipment. Mechanical vibrations cause magnetic flux interference by changing the angle of the dipstick and thus the SQUID with respect to the magnet. To minimize this interference, the dewar is placed on a mechanically damped platform and has only flexible connections to the gas handling system and the mains-fed electronics. The remaining flux interference is compensated by operating the stripline in a feedback loop which maintains a constant average output voltage across the SQUID.

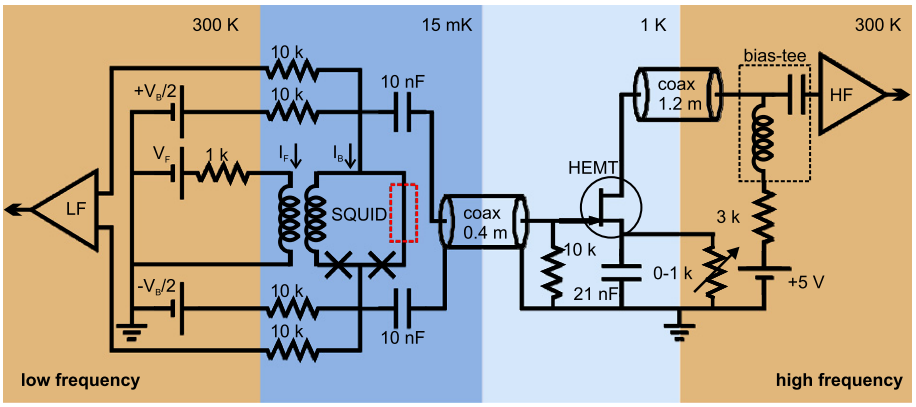

Fig. 4. Schematic of the amplification stages and control electronics at the various temperatures. The dc SQUID is connected to the low-frequency biasing electronics on the left side via 10 kΩ resistors and is connected to the high-frequency amplifier through capacitors to prevent dc currents from running between the low- (<10 kHz) and high-frequency (MHz) sides. The first high-frequency amplification stage is a High Mobility Electron Transistor (HEMT), mounted on the 1 K plate of the refrigerator. A 10 kΩ bleed resistor connects the gate to ground. A room temperature voltage source and tunable resistor are used to bias the transistor in a common source configuration. The amplified voltage is measured using a second, room temperature amplifier connected to the drain of the HEMT, with a bias-tee to separate the dc bias and the high-frequency signal.

will be coupled back into the SQUID by the feedback loop. The feedback loop operates at frequencies up to 1 kHz and thus does not influence the high-frequency oscillations due to the micromechanical resonator (MHz range). The optimized setup stabilizes the flux to a standard deviation of $0.01\Phi_0$.

2.2. Cryogenic high-frequency amplifier

The measurement imprecision is determined by the total noise that is added to the displacement of the resonator by all the amplification stages. Ideally the first transducer, the dc SQUID in this case, should be the dominant noise source. Note that the dc SQUID can in principle be a quantum limited flux [15] and position [16] detector.

In previous work [12] the first voltage amplifier was at room temperature and its noise was dominant, with an equivalent input noise level of 0.30 nV Hz at 2 MHz at the amplifier input. As this level is partly determined by Johnson noise of the transistor channel, it should decrease when the operating temperature of the amplifier is lowered. Another important factor is the signal loss from the SQUID to the amplifier due to the parasitic capacitance of the coaxial cable which was several meters in length. The loss of gain was estimated to be almost an order of magnitude, which means that the actual equivalent input noise level at the SQUID was around 3 $\mathrm{nV/Hz^{1/2}}$. This loss can be decreased by mounting the amplifier closer to the SQUID. For these two reasons, we have mounted a High Electron Mobility (HEMT) amplifier on the 1 K stage of the dilution refrigerator, using a phosphor-bronze core coaxial cable with a length of 0.4 m to connect the HEMT to the SQUID (Fig. 4).

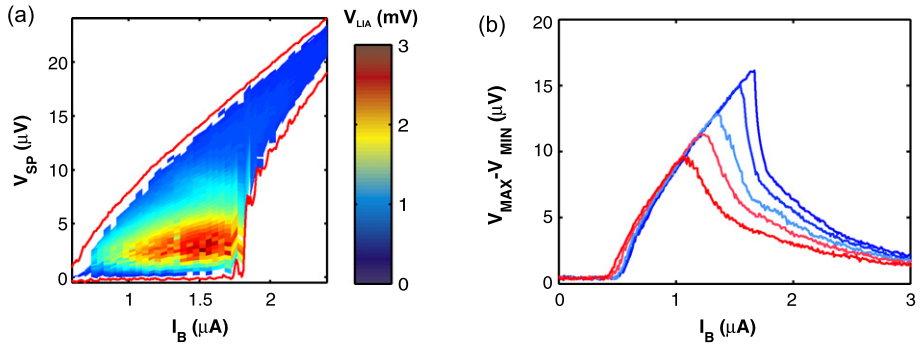

Fig. 5. (a) Map of the lock-in voltage V_{LIA} as a function of I_B and voltage setpoint V_{SP}. V_{LIA} is proportional to V_Φ and is used to normalize the measured resonator spectra. (b) The voltage swing $V_{\mathrm{MAX}} - V_{\mathrm{MIN}}$ as a function of I_B at temperatures ranging from 15 mK (blue) to 420 mK (red). I_C^{MAX} is always at the maximum voltage swing and I_C^{MIN} is the lowest current at which the swing is non-zero.

The HEMT is used as a common-source, high-input-impedance amplifier [17]. The variable resistor in Fig. 4 is used to set the bias current through the HEMT. The amplifier has a maximum signal-to-noise ratio when it is tuned to its maximum gain point, which is found for a bias current of 0.8 mA. At room temperature the output of the HEMT is further amplified by a high-impedance JFET amplifier with a gain of 1.7×10^3 V/V at 2 MHz. When the dilution unit is in operation and the HEMT is cold (1–4 K) it has a gain of 10 V/V, which was determined by replacing the SQUID with a 1 kΩ resistor and measuring its Johnson noise as a function of temperature. The SNS junctions of the SQUID cannot be used for this purpose, even though they also produce Johnson noise. They have a normal-state resistance R on the order of 10 Ω and at millikelvin temperatures, their contribution to the noise is much smaller than that of the HEMT amplifier. The total gain of the high-frequency amplifiers is thus $G_{HF} = 1.7 \times 10^4$ V/V.

The noise power at the output of the JFET amplifier is $S_{V_n}^{1/2} = 4.5$ μV/Hz$^{1/2}$, with the dominant noise contribution coming from the HEMT. This gives an equivalent input noise of 0.26 nV/Hz$^{1/2}$ at the SQUID, over an order of magnitude better than the previous configuration [12]. Surprisingly, the noise floor at the HEMT input is similar to the same HEMT at room temperature. The major improvement is thus due to a reduction of capacitive losses.

3. Motion detection

3.1. dc SQUID measurements

During acquisition of the mechanical resonator signal, the SQUID is operated in a feedback loop, which means that the voltage setpoint V_{SP} is specified instead of Φ. In order to find the optimum gain point and to measure other properties such as the mechanical resonance frequency, we must first determine the values in V_{SP}–I_B space for which the feedback loop produces a stable lock. This is done by taking the minimum and maximum voltage, V_{MIN} and V_{MAX}, as a function of I_B from measurements like that shown in Fig. 2. The feedback loop is operated within this region (between the red lines in Fig. 5(a)), and at each bias point, the flux gain is measured in addition to either the driven response or the noise spectrum of the resonator.

The flux gain V_Φ is measured by applying a small sinusoidal current signal to the stripline at 5 kHz. The corresponding response of the SQUID is measured using a lock-in amplifier which is connected to the low-frequency side of the measurement circuit (Fig. 4). V_Φ is related to the measured amplitude V_{LIA} according to

$$V_{LIA} = \frac{V_{IF} M_{STRIP} G_{LF}}{A_{IF} R_{IF}} V_\Phi \tag{7}$$

where $M_{STRIP} = 16$ pH is the mutual inductance between the stripline and the SQUID loop (Fig. 2(b)). $V_{IF} = 0.85$ V is the RMS output voltage of the lock-in amplifier which is attenuated by a factor $A_{IF} = 4$ kV/V by the input circuit of the battery-fed electronics (Fig. 3) and applied to a 1 kΩ resistor, R_{IF}, which is placed in series with the stripline. This couples a small flux signal of 6.5 mΦ_0 into the loop. The SQUID output voltage is then amplified by the low-frequency amplifier by a factor $G_{LF} = 10$ kV/V. Since only V_Φ depends on the SQUID bias parameters (and temperature), V_Φ is determined by measuring V_{LIA} and using Eq. (7). Fig. 5(a) shows V_{LIA} as a function of SQUID bias. The highest flux gain occurs at low voltage setpoints, as expected from Fig. 2. By using the parameters mentioned above and the maximum $V_{LIA} = 3$ mV from Fig. 5, the maximum flux gain is found to be $V_\Phi = 176$ μA/Φ_0.

The minimum and maximum critical currents, I_C^{MIN} and I_C^{MAX} decrease for increasing temperatures, Fig. 5(b). For the temperature-dependence measurements, it is therefore important to track the critical currents and the voltage swing in order to keep the setpoint of the feedback loop within the stable region. The flux gain V_Φ depends on I_C and thus also decreases with increasing temperature. As the value of V_Φ is needed to calibrate the displacement sensitivity, V_{LIA} is measured with each resonator spectrum. This calibration is described in the next section.

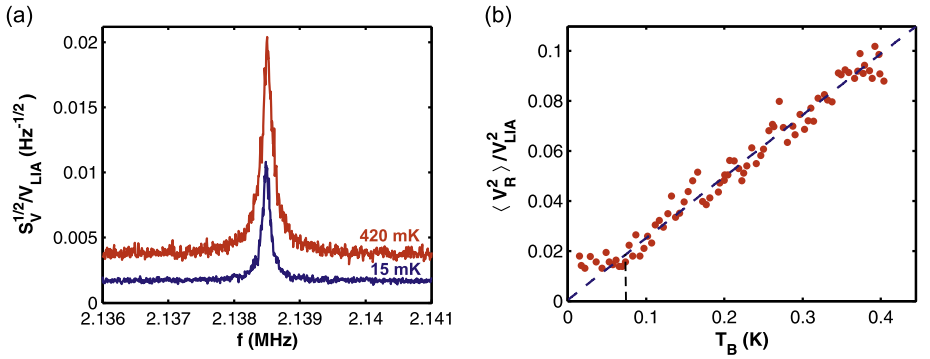

Fig. 6. (a) Normalized voltage noise spectra at 15 mK (blue) and 420 mK (red). The Lorentzian peaks are due to the Brownian motion of the resonator and the integrated area under the curves is proportional to the root-mean-square motion of the resonator which is in turn proportional to the substrate temperature according to the equipartition theorem. The area under the red curve is clearly larger than under the blue curve. The measurement sensitivity is determined by the flat noise floor away from the resonance peak and is also lower at decreased temperature. (b) Normalized integrated noise power plotted as a function of refrigerator temperature. The noise power decreases linearly with temperature down to a saturation temperature of 70 mK (black vertical line). A linear fit of the data above the saturation temperature (blue line) yields a slope which is used to calculate the displacement-to-voltage gain of the SQUID position detector. This is in turn used to convert the measured noise spectra from voltage noise to displacement noise.

3.2. Displacement calibration

A reference is needed in order to calibrate the responsivity $\frac{\partial V_{SQ}}{\partial u}$ of the combined dc SQUID position detector and amplifier chain. Thermal energy is a natural choice because the equipartition theorem relates the mean-square position fluctuations of the resonator $\langle u^2\rangle$ to its temperature T_R. By using Eq. (2), the integrated voltage noise power due to the motion of the resonator becomes

$$\langle V_R^2\rangle = \left(\frac{\partial V_{SQ}}{\partial u}\right)^2 \langle u^2\rangle = \left(\frac{\partial V_{SQ}}{\partial u}\right)^2 \frac{k_B T_R}{k_R} \tag{8}$$

The total voltage noise has an additional white noise floor S_{V_n} due to the detector and the amplifiers. When this noise is referred back to the resonator displacement, i.e.

$$S_{u_n} = S_{V_n}\left(\frac{\partial V}{\partial u}\right)^{-2} \tag{9}$$

it is known as the displacement sensitivity or imprecision noise. The imprecision noise is related to the displacement resolution $\sqrt{\langle u_n^2\rangle}$ of the detector according to [6]

$$\langle u_n^2\rangle = S_{u_n}\frac{\pi f_R}{2Q_R} \tag{10}$$

In order to examine the quantum limit for linear detection, the resolution should be tunable to be less than $\sqrt{\langle u^2\rangle_{QL}}$ (Eq. (3)).

Fig. 6(a) shows the voltage noise spectrum around the resonance frequency, measured at two different temperatures. As was mentioned in the previous subsection, the flux gain of the SQUID changes with temperature and therefore, to compare displacement noise spectra at different temperatures, they must be normalized by V_Φ. For this reason V_{LIA}, which is proportional to V_Φ, is measured after each spectrum and the spectra are normalized by V_{LIA}. As can be seen in Fig. 6(a), the integrated area under the spectra, $\langle V_R^2\rangle/V_{LIA}^2$, is larger for the higher temperature, as is expected from Eq. (8). Another observation is that the normalized noise floor is lowest at low temperatures. This is because the dominant noise source is the HEMT amplifier and although its noise does not depend on the bath temperature T_B, the flux gain V_Φ decreases with increasing T_B, thereby increasing the noise level when it is referred back to the resonator displacement.

Although one could calculate $\frac{\partial V_{SQ}}{\partial u}$ from a single spectrum by using Eq. (8), this assumes that the temperature of the resonator T_R is the same as the temperature of the bath T_B, which is measured by a separate thermometer. At temperatures below 1 K, this point is not trivial and many groups observe a saturation of T_R, where it no longer follows T_B for varying reasons, such as on-chip power dissipation and back-action of the displacement detector [7,14]. The responsivity can be more accurately determined by measuring $\langle V_R^2\rangle/V_{LIA}^2$ as a function of T_B. From Eq. (8), a linear relationship between these two quantities is expected as long as $T_R = T_B$. Then, $\frac{\partial V_{SQ}}{\partial u}$ can be determined by calculating the slope $\frac{\mathrm{d}\langle V_R^2\rangle/V_{LIA}^2}{\mathrm{d}T_B}$ and using

$$\frac{\partial V}{\partial u}(T_B) = \sqrt{\frac{k_R}{k_B}\left(\frac{\mathrm{d}\langle V_R^2\rangle/V_{LIA}^2}{\mathrm{d}T_B}\right)}V_{LIA}(T_B) \tag{11}$$

Here, $\frac{\partial V}{\partial u}$ at temperature T_B is stated explicitly as consisting of the parameters within the square root, which are approximately temperature independent and V_{LIA}, which depends strongly on T_B. By combining Eqs. (3), (9), (10) and (11), the position resolution with respect to the quantum limit can be expressed in terms of only measured quantities and natural constants:

$$\sqrt{\frac{\langle u_n^2\rangle}{\langle u_{QL}^2\rangle}} = \sqrt{\frac{k_B S_{V_n}}{2\hbar Q_R}\left(\frac{\mathrm{d}\langle V_R^2\rangle/V_{LIA}^2}{\mathrm{d}T_B}\right)^{-1}}\left(\frac{1}{V_{LIA}(T_B)}\right) \tag{12}$$

Note that Q_R and V_{LIA} both depend on temperature and will be maximal at the lowest bath temperatures T_B. This is where the best resolution is achieved.

Fig. 6(b) shows the thermal calibration for the dc SQUID detector. The optimum bias point is determined by finding the maximum gain in Fig. 5. The bias is defined in relative terms: $I_B = I_C^{\mathrm{MIN}} + 0.8(I_C^{\mathrm{MAX}} - I_C^{\mathrm{MIN}})$ and $V_{SP} = V_{\mathrm{MIN}} + 0.3(V_{\mathrm{MAX}} - V_{\mathrm{MIN}})$ because these values change with temperature and must be tracked, as was explained in the previous subsection. For this purpose, the SQUID is calibrated at each temperature point. From a linear fit to the data in Fig. 6(b), the slope $\frac{\mathrm{d}\langle V_R^2\rangle/V_{LIA}^2}{\mathrm{d}T_B} = 0.25\ \mathrm{K}^{-1}$ is obtained. The resonator temperature saturates around $T_R = 70$ mK, which corresponds to an average occupation of 6.8×10^2 phonons. This is similar to what was observed in previous work [12]. At $T_B = 15$ mK, we measure $V_{LIA} = 3$ mV and $Q_R = 3 \times 10^4$. Combined with the output noise floor $\sqrt{S_{V_n}} = 4.5\ \mu\mathrm{V/Hz}^{1/2}$ which was mentioned in Section 2 and the spring constant $k_R = 110$ N/m from Section 1, this yields $\frac{\partial V}{\partial u} = 4.2\ \mu\mathrm{V/fm}$ and $\sqrt{\frac{\langle u_n^2\rangle}{\langle u_{QL}^2\rangle}} = 4.4$ or in absolute terms, $\sqrt{S_{u_n}} = 1\ \mathrm{fm/Hz}^{1/2}$. As discussed in Section 2, this is an order-of-magnitude improvement over previous work [12] is achieved by placing the HEMT amplifier closer to the SQUID at the 1 K stage of the dilution refrigerator.

A further improvement of the displacement resolution is possible by increasing the flux responsivity of the SQUID and by using an amplifier with an even lower noise floor, such as a second SQUID. With these improvements, one should be able to push the SQUID displacement sensitivity beyond the standard quantum limit, where detector back-action becomes the dominant source of fluctuations. Since the back-action in this SQUID-based detection scheme is tunable [13], it is an interesting system to study in more detail. For example, it may become possible to go from a regime where the SQUID is cooling the resonator to a regime where the resonator oscillation is amplified, possibly to the point of self-sustained oscillation [18]. Because of their small mass and low dissipation, embedded micro- and nanomechanical resonators are an excellent platform to study these effects.

Acknowledgements

The authors thank I. Mahboob, T. Akazaki, H. Okamoto and K. Yamazaki for help with fabrication, R. Schouten for the measurement electronics and M. van Oossanen for the vibration damping setup. This work was supported in part by JSPS KAKENHI (20246064 and 18201018), FOM, NWO (VICI grant) and a EU FP7 STREP project (QNEMS).

References

[1] S. Verbridge, H. Craighead, J. Parpia, A megahertz nanomechanical resonator with room temperature quality factor over a million, Applied Physics Letters 92 (2008) 013112.
[2] C. Caves, K. Thorne, R. Drever, V. Sandberg, M. Zimmermann, On the measurement of a weak classical force coupled to a quantum-mechanical oscillator. I. Issues of principle, Reviews of Modern Physics 52 (2) (1980) 341–392.
[3] M. Poot, H. S. J. van der Zant, Mechanical systems in the quantum regime, Physics Reports (2011), in press, arXiv:1106.2060v2.
[4] A. O'Connell, M. Hofheinz, M. Ansmann, R. Bialczak, M. Lenander, E. Lucero, M. Neeley, D. Sank, H. Wang, M. Weides, et al., Quantum ground state and single-phonon control of a mechanical resonator, Nature 464 (7289) (2010) 697–703.
[5] R. Knobel, A. Cleland, Nanometre-scale displacement sensing using a single electron transistor, Nature 424 (6946) (2003) 291–293.
[6] M. LaHaye, O. Buu, B. Camarota, K. Schwab, Approaching the quantum limit of a nanomechanical resonator, Science 304 (5667) (2004) 74.
[7] N. Flowers-Jacobs, D. Schmidt, K. Lehnert, Intrinsic noise properties of atomic point contact displacement detectors, Physical Review Letters 98 (9) (2007) 96804.
[8] A. Cleland, J. Aldridge, D. Driscoll, A. Gossard, Nanomechanical displacement sensing using a quantum point contact, Applied Physics Letters 81 (2002) 1699.
[9] G. Anetsberger, O. Arcizet, Q. Unterreithmeier, R. Rivière, A. Schliesser, E. Weig, J. Kotthaus, T. Kippenberg, Near-field cavity optomechanics with nanomechanical oscillators, Nature Physics 5 (12) (2009) 909–914.
[10] J. Teufel, T. Donner, M. Castellanos-Beltran, J. Harlow, K. Lehnert, Nanomechanical motion measured with an imprecision below that at the standard quantum limit, Nature Nanotechnology 4 (12) (2009) 820–823.
[11] J. Clarke, A. Braginski, The SQUID Handbook, Wiley-Vch, 2006.
[12] S. Etaki, M. Poot, I. Mahboob, K. Onomitsu, H. Yamaguchi, H. Van der Zant, Motion detection of a micromechanical resonator embedded in a dc SQUID, Nature Physics 4 (10) (2008) 785–788.
[13] M. Poot, S. Etaki, I. Mahboob, K. Onomitsu, H. Yamaguchi, Y.M. Blanter, H.S.J. van der Zant, Tunable backaction of a dc SQUID on an integrated micromechanical resonator, Physical Review Letters 105 (20) (2010) 207203.
[14] A. Naik, O. Buu, M. LaHaye, A. Armour, A. Clerk, M. Blencowe, K. Schwab, Cooling a nanomechanical resonator with quantum back-action, Nature 443 (7108) (2006) 193–196.

[15] R. Koch, D. Van Harlingen, J. Clarke, Quantum noise theory for the dc SQUID, Applied Physics Letters 38 (5) (2009) 380–382.
[16] M.P. Blencowe, E. Buks, Quantum analysis of a linear dc squid mechanical displacement detector, Physical Review B 76 (1) (2007) 014511, doi:10.1103/PhysRevB.76.014511.
[17] P. Horowitz, W. Hill, The Art of Electronics, Cambridge University Press, 2001.
[18] X. Feng, C. White, A. Hajimiri, M. Roukes, A self-sustaining ultrahigh-frequency nanoelectromechanical oscillator, Nature Nanotechnology 3 (6) (2008) 342–346.
[19] H. Takayanagi, T. Kawakami, Superconducting proximity effect in the native inversion layer on InAs, Physical Review Letters 54 (22) (1985) 2449–2452.